

Development and testing of novel catalyst-coated membrane with platinum free catalysts for alkaline water electrolysis

Jaromír Hnát,^{*a} Michaela Plevová,^a Ramato Ashu Tufa,^a Jan Zitka,^b Martin Paidar,^a and Karel Bouzek^a

^a Department of Inorganic Technology, University of Chemistry and Technology Prague, Technická 5, 16628 Prague 6, Czech Republic

^b Institute of Macromolecular Chemistry of the Academy of the Sciences of the Czech Republic, Heyrovského Sq.2, 16206 Prague 6, Czech Republic

Abstract

A stable, non-platinum-catalyst-coated anion-exchange membrane with a promising performance for alkaline water electrolysis as an energy conversion technology is prepared and tested. Hot plate spraying technique is used to deposit electrodes on surface of the anion selective polymer electrolyte membrane in the thicknesses of 35 and 120 μm corresponding to the catalyst load of 2.5 and 10 mg cm^{-2} . The platinum free catalysts based on NiCo_2O_4 for anode and NiFe_2O_4 for cathode were used together with anion selective polymer binder in the catalyst/binder ratio equal to 9:1. The performance of the prepared membrane electrode assembly is verified under the conditions of the alkaline water electrolysis using different concentrations of the liquid electrolyte ranging from 1 to 15 wt.% KOH. The electrolyser performance is compared to the cell utilising the catalyst coated Ni foam as electrodes. The prepared membrane-electrode assembly stability at a current load of 250 mA cm^{-2} is verified by an electrolysis test lasting for 72 hours. Results of the experiments provided indicate a possibility of the significant catalyst loading reduction when compared to the catalyst coated electrode approach.

Keywords: catalyst coated membrane; alkaline environment; water electrolysis; non-platinum catalysts; anion exchange membrane

DOI: 10.1016/j.ijhydene.2019.05.054

© 2019. This manuscript version is made available under the CC-BY-NC-ND 4.0 license <http://creativecommons.org/licenses/by-nc-nd/4.0/>

Highlights

- Stable catalyst coated membrane for alkaline water electrolysis was prepared.
- Non-Pt catalyst used on cathode and anode side.
- Significant decrease in the catalyst load was achieved, while maintaining the performance.
- Stability proven for 72 hours under realistic alkaline water electrolysis conditions.

1 Introduction

Hydrogen represents a clean, efficient and versatile energy carrier that can be deployed for energy supply, environmental protection and for the sustainable development of society. It can, in fact, be produced indefinitely by water electrolysis using electricity from renewable energy resources. Water electrolysis is a mature and flexible approach to relatively simple sustainable hydrogen production driven by a surplus of renewable energy resources. In particular, alkaline water electrolysis (AWE), operating with relatively cheap and non-noble electrocatalysts, enables the development of cost-effective and high performance AWE systems [1, 2]. The AWE technology currently operated can be improved by the development of electrode materials with low overpotential [3-6] or by using alkaline polymer electrolyte membrane separators [1, 7-9]. Between the promising non-platinum materials the catalyst based on Ni [10-12], NiCo [13, 14] or Co [15, 16] can be used in alkaline water electrolysis with high efficiency. The application of a sufficiently conductive and stable anion-selective polymer electrolyte membrane enables the design of alkaline polymer electrolyte water electrolysis (APWEL) system similar to proton-exchange membrane (PEM) technology. Such an APWEL system can be operated using a liquid electrolyte of low concentration. If the polymer electrolyte used is also accessible in the form of a stable and conductive catalyst layer binder, even demineralized water can be circulated through the system [1, 7-9]. However, due to the problems with the membrane CO₂ poisoning, which is caused by the formation of the HCO₃⁻ or CO₃²⁻ ions and their negative influence on the ionic conductivity of the anion selective polymer membrane due to the blockage of the

functional groups and limited stability of the used materials, e.g. Ni, at $\text{pH} < 9$ this approach is not really feasible at present time. On the other hand, even relatively low concentrated ($w > 1 \text{ wt.}\%$) solutions of KOH can absorb the air CO_2 protecting thus the membrane from poisoning and establish $\text{pH} > 9$, which is necessary from the Ni stability point of view.

The membrane-electrode assembly (MEA) is a core component of APWEL. The design of the MEA strongly influences the degree of catalyst utilization and electrolyte concentration needed to maintain high system efficiency. The design of high-quality MEAs thus has a direct impact on the performance, cost and durability of the resulting APWEL systems. Therefore, mass production of a high-quality MEA is critical for the commercial implementation of this technology. In principle, two methods of MEA production are known from PEM technology: (i) catalyst-coated substrate (CCS, sometimes also called a catalyst-coated electrode) [3, 5, 17, 18] and (ii) catalyst-coated membrane (CCM) [19].

Although for PEM water electrolysis technology the CCM is the preferred approach, providing more effective catalyst utilization and process intensity for APWEL, the CCS is the sole MEA production technique in use so far. This is mainly on account of the limited stability of the alkaline polymer electrolyte, especially in the case of the catalyst layer binder. By depositing a catalytic layer on the substrate of the gas diffusion layer (GDL) this problem can be avoided, *e.g.* by using PTFE as an alternative, highly stable binder. The main disadvantage of this approach is the limited contact between the catalyst and the polymer electrolyte membrane, as they are in direct contact in places where the GDL touches the membrane surface. Due to the absence of a microporous layer, this contact constitutes only a small percentage of the membrane surface, typically less than 10 %.

On the other hand, CCM approach circumvents this problem. Catalyst has ideal contact with the membrane, thus ensuring high process efficiency together with efficient catalyst utilization and, therefore, lower catalyst loading [20, 21]. The polarization and ohmic resistances between the catalytic layer and the membrane can also be attenuated, thus ultimately improving the performance of CCM-based MEAs (CCM-MEA). Experience gained in PEM technology shows that the CCM-MEA can be fabricated by several methods, including doctor blade/decal transfer, hand painting, air spraying, pulse spray swirl, rolling, ultrasonic spray deposition, and inkjet/screen printing [21-31].

Whereas the CCM-MEA has been intensively studied for PEM fuel cells (PEMFC) [32-41], direct methanol fuel cells (DMFC) [42-44] and PEM electrolyzers [44-49] to advantage, there is a lack of similar investigations for an alkaline environment due to the absence of an appropriate anion-selective polymer binder. To our knowledge, the only study evaluating the performance CCM-MEAs is that of Leng *et al.*, who coated the surfaces of a commercial A201 membrane (Tokuyama Corp., Japan) with IrO₂ catalytic ink (loading: 2.9 mg/cm²) and Pt catalytic ink (loading: 3.2 mg/cm²), using AS-4 ionomer (Tokuyama Corp., Japan) as a binder on the anode and cathode sides, respectively [50]. The second option reported is aminated poly(sulfone). Rapid MEA degradation was observed in the first hours, followed by a type of plateau lasting for varying amounts of time before the cell collapsed. Unfortunately, the authors provide neither a clear discussion of the MEA degradation mechanism, nor information on the stability of the catalytic layer on the membrane surface, *e.g.* by SEM analysis. Moreover, this work utilized expensive precious catalysts, thus eliminating one of the main advantages of APWEL over PEM water electrolysis. Recently, Ito *et al.* [51] prepared a catalyst-coated membrane using identical materials, *i.e.* A201 membrane and AS-4 ionomer binder (Tokuyama Corp., Japan) with a commercial, non-precious catalyst from

Acta S.P.A., deposited on both sides. This system proved to be unstable on the anode side. The catalytic layer peeled off the membrane quite readily. This finding indicates that, as in the previous case [50], the main issue was the quality of the anode adherence and contact with the membrane.

With the respect to the data published in literature, the present study is unique in utilization of non-precious catalysts for preparation of CCM-MEA for APWEL and showing high stability of both anode and cathode catalysts layers. It used, to advantage, a novel alkaline polymer electrolyte based on a polystyrene-block-poly(ethylene-ran-butylene)-block-polystyrene (PSEBS) membrane with 1,4-diazabicyclo[2.2.2]octane (DABCO) functional groups which had recently been prepared by our group [52]. Mixed oxides with a spinel structure were used as catalysts. CCMs were prepared by the spray coating method. In the next step prepared CCMs were investigated with respect to their morphology and electrochemical properties under conditions of APWEL in a laboratory-scale alkaline water electrolyser. The results obtained indicate the unique compatibility of the catalyst layers with the membrane, which have not been reported yet and promising results in terms of performance and stability.

2 Experimental part

2.1 Materials

The Ni foam used for electrodes production was obtained from INCO Advanced Technology Materials (Dalian) Co., Ltd (average pore size 580 μm), thickness 2 mm. The circulating electrolyte was produced using potassium hydroxide (KOH) (85%, PENTA, Czech Republic).

Polystyrene-block-poly(ethylene-ran-butylene)-block-polystyrene (PSEBS) ($M = 0.21$ (butylene), $N = 0.67$ (ethylene), $blc = 0.12$ (styrene)), (Sigma Aldrich), $M_w = 118,000$ g mol^{-1} , zinc chloride anhydrous (Lachema, Czech Republic), dimethoxymethane (DMOM) ($\geq 99\%$, Sigma Aldrich), phosphorus trichloride (99% , Sigma Aldrich), chloroform (LachNer, Czech Republic, (p.a), toluene (LachNer, Czech Republic, (p.a), ethanol (technical grade) and 1,4-diazabicyclo[2.2.2]octane (DABCO) ($\geq 99\%$, Sigma Aldrich) were used for the polymer electrolyte production.

Sodium hydroxide (NaOH) (99% , PENTA, Czech Republic), cobalt nitrate hexahydrate ($\text{Co}(\text{NO}_3)_2 \cdot 6\text{H}_2\text{O}$) ($\geq 99\%$, PENTA, Czech Republic), nickel nitrate hexahydrate ($\text{Ni}(\text{NO}_3)_2 \cdot 6\text{H}_2\text{O}$) ($\geq 99\%$, PENTA, Czech Republic) and iron chloride (FeCl_3) ($\geq 98\%$, PENTA, Czech Republic) served for the catalyst production.

All chemicals were used as received.

2.2 Catalyst preparation

Non-precious catalysts were prepared by the co-precipitation method, which is described in detail elsewhere [5, 53]. In brief, for the NiCo_2O_4 anode catalyst, a stoichiometric amount of cobalt nitrate hexahydrate and nickel nitrate hexahydrate was dissolved in water. NaOH solution (2 mol dm^{-3}) was added under stirring. The black precipitate was filtered off, washed and calcined at a temperature of 325°C for 4 hours under air atmosphere. Temperature increase rate was 4°C min^{-1} . For the NiFe_2O_4 cathode catalyst, the same procedure was used, starting from nickel nitrate hexahydrate and iron chloride. In this case, calcination was performed at 475°C for 4 hours, again in air atmosphere.

2.3 Synthesis of polymer materials

The detailed procedure of the membrane synthesis was described elsewhere [52]. The synthesis proceeded in several steps starting with the PSEBS chlorination reaction

through the reaction of DMOM with phosphorous trichloride and ZnCl_2 in 5 wt.% solution of PSEBS in order to prepare chloromethylated PSEBS (PSEBS-CM). The product was filtered off, washed with ethanol and dried. Membrane was casted out of this material.

In the second step, the PSEBS-CM membrane was immersed in 10 wt.% solution of DABCO in ethanol for 72 hours at room temperature to obtain the functionalized anion selective polymer membrane with attached DABCO functional groups (PSEBS-CM-DABCO).

2.4 Membrane pre-treatment

Prior to deposition of the catalytic layers on the membrane's surface, the membranes were pre-treated in order to ensure its reproducible activation. The activation procedure consisted in immersing membrane samples in the solutions of 0.1 mol dm^{-3} NaOH and 0.1 mol dm^{-3} HCl for defined time intervals. Between the individual immersions, the membrane was carefully washed in demineralized water. For more details on the activation procedure see [52].

2.5 MEA preparation

The MEAs were produced using a hot spraying technique. The catalyst ink was prepared by mixing the corresponding catalysts with 5 wt.% solution of PSEBS-CM in chloroform (CHCl_3). This catalytic ink composition was obtained as an optimal one for catalyst coated substrate membrane electrode assembly (CCS-MEA) [54]. The catalyst ink was sprayed either on the nickel (Ni) foam electrode (for CCS-MEA) or directly on the surface of the membrane (for CCM-MEA). Both substrates were heated to 50°C in order to accelerate the evaporation of the solvent. The CCS-MEA was prepared with catalyst load 10 mg cm^{-2} as well as first CCM-MEA. The value of catalyst load was evaluated as optimal in our previous study [54] and thus it was adopted for CCM-MEA at the first step. In the next step, the catalyst load for CCM-MEA was decreased to 2.5

mg cm⁻². After deposition of the appropriate amount of catalysts (the load of the anode and cathode catalyst was identical in all cases), substrates with the catalytic layer were immersed in the 10 wt.% solution of DABCO in ethanol for 24 hours at room temperature in order to functionalize the polymer and to obtain PSEBS-CM-DABCO.

2.6 MEA characterization

The morphology of the prepared CCM-MEA, as well as the quality of the contact on the interface between the membrane and the electrode, were investigated prior to, and after the alkaline water electrolysis experiment, using a Hitachi S4700 scanning electron microscope.

Alkaline water electrolysis was performed by recording the load of the curves at 45 °C in 10 wt.% (1.95 mol dm⁻³) KOH solution and a flow rate of 5 ml min⁻¹. Load curves were recorded in a voltage range of 1.5 to 2.0 V. The CCM-MEA stability was verified in water electrolysis during operation at a current load of 250 mA cm⁻². A laboratory test station was coupled with an electrochemical impedance spectroscopy measurement (EIS) system using a Solartron SI 1250 frequency Response Analyser and a Solartron SI 1287 electrochemical interface. The spectra were recorded in a two-electrode arrangement at open circuit potential (system resistivity (R_s) determination) and at 1.8 V (polarization resistance (R_p) determination) within a frequency range of 65 kHz – 1 Hz with perturbing signal amplitude of 20 mV. The equivalent circuits used for the EIS spectra evaluation is shown in Fig. 1. Two different equivalents circuits were used as some of the measured spectra contained one or two time constants.

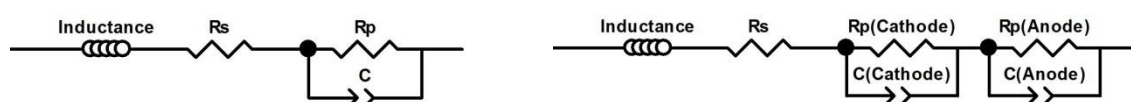


Fig. 1: Equivalent electrical circuits used for the evaluation of the electrochemical impedance spectra. R_s – system resistivity, R_p – polarisation resistance, C – constant phase element.

3 Results and Discussion

3.1 CCM-MEA mechanical stability

With respect to the quality of the contact between the catalytic layer and the membrane, Fig. 2 shows the SEM cross-sections of the CCM-MEA as prepared (Fig. 2A, C) and after the alkaline water electrolysis experiment (Fig. 2B, D), including a load curve recording and an additional 20 hours of operation at a constant current load of 250 mA cm⁻². As can be seen in Fig. 2A, the average thickness of the catalytic layer corresponds to approximately 35 µm for a catalyst load of 2.5 mg cm⁻². In the case of the CCM with a catalyst load of 10 mg cm⁻², the average thickness is approximately 120 µm. The SEM pictures clearly document excellent contact between the catalytic layer and the surface of the membrane. This is especially true in the case of a thinner catalytic layer, i.e. lower catalyst load. No signs of delamination are visible, not only for the freshly prepared CCM-MEA, but also for the CCM-MEA after the electrolysis test, see Fig. 2B. Even under the harsh conditions of anodic oxygen evolution, the ionomer binder was able to maintain the required mechanical properties and prevent removal of catalyst from the catalytic layer as well as its delamination from the membrane surface.

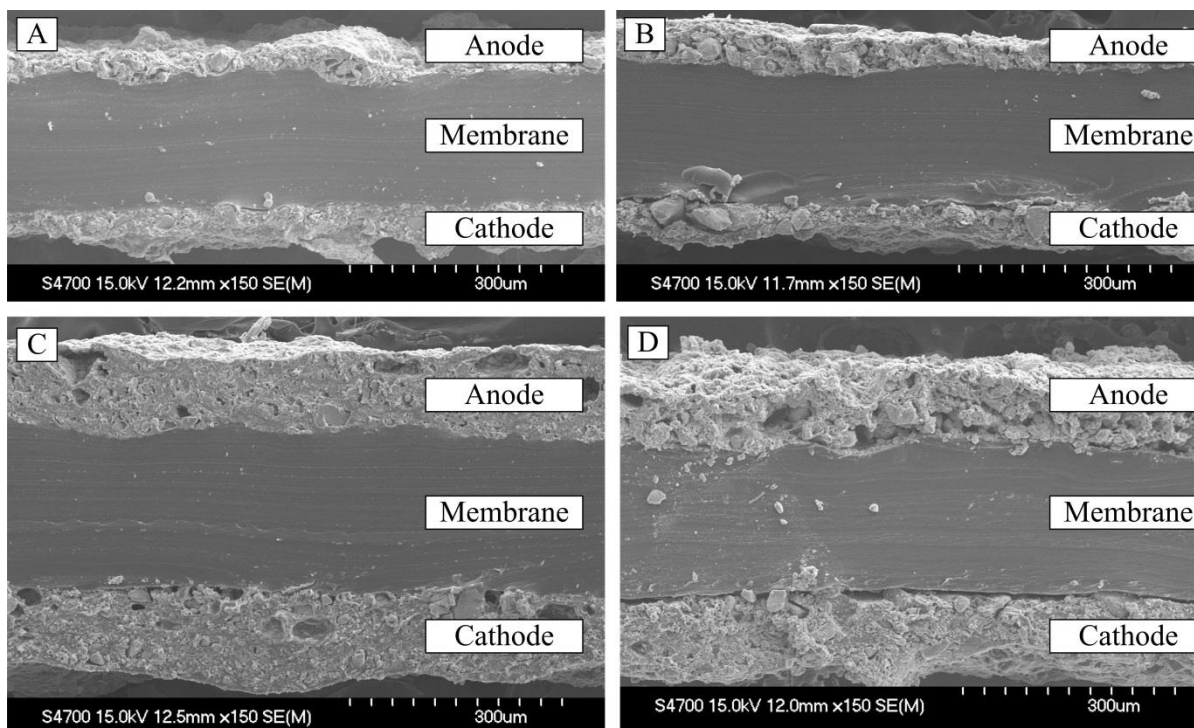


Fig. 2: Cross-section of the prepared CCMs before (Fig. 2A, C) and after (Fig. 2B, D) an APWEL test. It includes load curve measurements in 10 wt.% KOH at 45 °C in a cell voltage range of 1.5 – 2.0 V with an additional 20 hours of constant current load 250 mA cm⁻². Catalyst load: 2.5 mg cm⁻² (A, B); 10 mg cm⁻² (C, D).

In the case of the thicker layer, i.e. higher catalyst load, the situation is different. The initial good contact of the catalytic layer with the membrane, documented by Fig. 2C, is disturbed by the electrolysis process and catalytic layer delamination becomes apparent, see Fig. 2D. Moreover, the thickness of the catalytic layer decreased and structure of the anode become partly loose. This can be attributed to the higher pressure of the evolved gases, mainly at the membrane-catalyst layer interface. The greater the thickness of the catalyst layer, the higher the mechanical stress in the system. On the anode side of MEA the reaction rate is slower and gas phase evolution is distributed more over the thickness of the catalytic layer. Therefore the morphology of this catalytic layer is partly disturbed also in its bulk. An additional aspect for both observed changes is the preparation of the sample for SEM inspection. During the breaking of the CCM-MEA, the thicker electrode is subjected to greater mechanical stress, which can result in delamination. A decrease in the thickness of the anode of about 8 % can be the result of an error during the

preparation of the CCM-MEA or it can be related to the poorer mechanical properties of the thicker layer and to the removal of some part of the catalyst. This is, of course, the point of further optimizing the preparation of the CCM-MEA and the composition of the catalyst layer. This assumption is supported by a fact, that no catalyst particles released from the catalytic layer were visually observed in the electrolyte solution/electrolyser hydraulic circuit during electrolysis for neither of both cases discussed at this place.

3.2 Comparison of CCS-MEA and CCM-MEA performance

The performance of CCM-MEAs and CCS-MEAs, compared in the form of alkaline water electrolysis load curves, is presented in Fig. 3A. In the first step, the same catalyst load of 10 mg cm^{-2} was used for both the CCM and the CCS system. A slightly better result was achieved with the CCM-MEA (10 mg cm^{-2}) configuration. However, the difference was negligible as the current densities at 2.0 V were 0.147 and 0.138 A cm^{-2} (increase about 6.5 %) for CCM-MEA (10 mg cm^{-2}) and CCS-MEA respectively. The reason for CCM-MEA (10 mg cm^{-2}) showed higher current density is better utilization of the catalyst. This is typical advantage of the CCM-MEA approach. In the next step, a loading of 2.5 mg cm^{-2} was used for CCM-MEA preparation. Surprisingly, this reduction in the loading had only an insignificant effect on the performance of the alkaline water electrolysis and was especially apparent at low current loads. At higher current loads it gradually attained the performance values observed for the higher catalyst load (the difference of the current densities for three compared MEAs was within $\pm 2.9 \%$). This may be explained by low conductivity of the catalytic layer, resulting in an inferior performance of the CCM-MEA with a loading of 10 mg cm^{-2} , compared to 2.5 mg cm^{-2} . This is supported by the shape of the load curves which, in the latter case, clearly display exponential behaviour. The more complex removal of gases

produced from the membrane-catalyst layer interface for the thicker catalyst layer may also play a certain role, as discussed above.

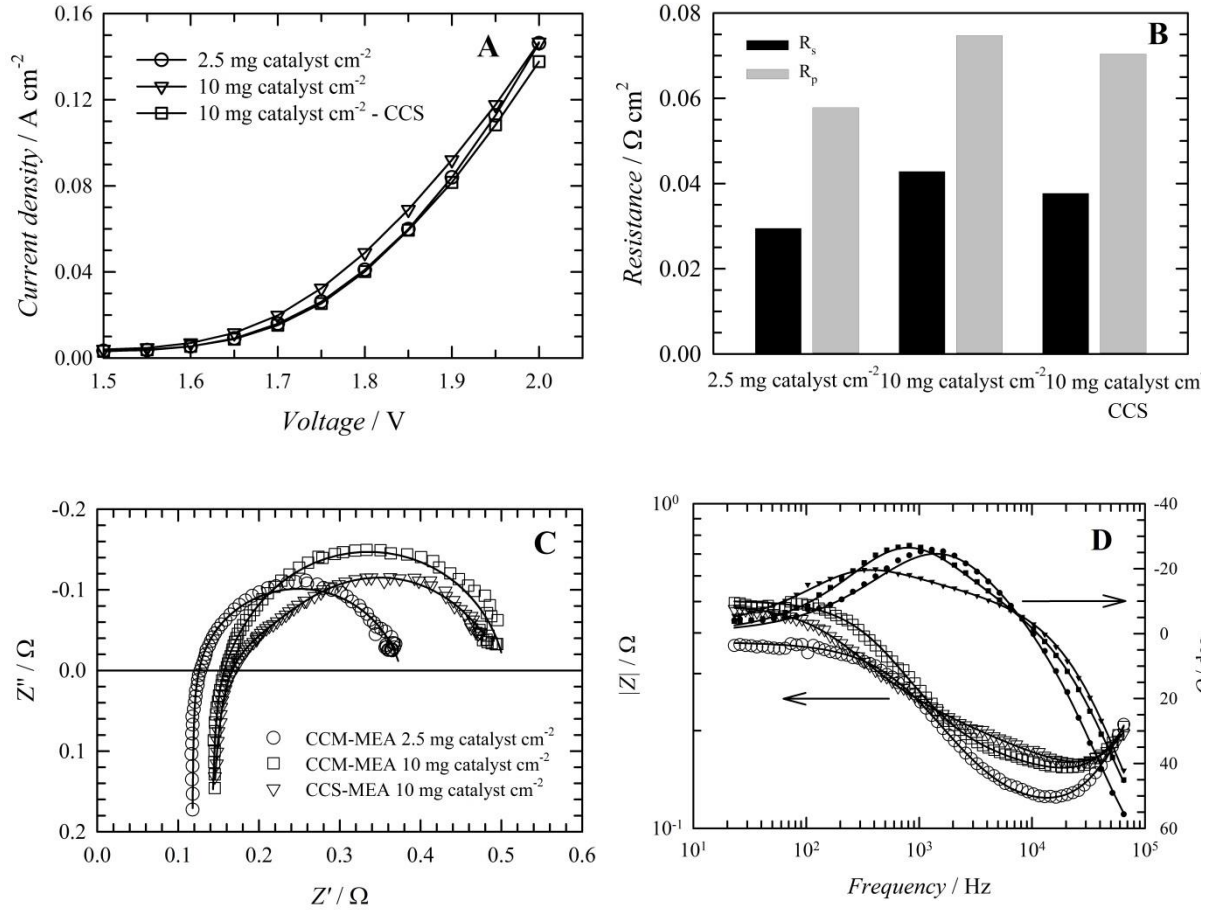


Fig. 3: (A) Load curves of APWEL using different MEAs (shown in figure inset, method of preparation is CCM if no other method is indicated). Geometrical area of the electrode 4 cm², temperature 45 °C, concentration of the liquid electrolyte 10 wt.%, electrolyte flow rate 5 ml min⁻¹. (B) Values of the R_s and R_p evaluated for particular MEAs configurations from EIS spectra. (C) Nyquist plot; (D) Bode plot – circle symbol corresponds to the CCM-MEA 2.5 mg catalysts cm⁻²; square symbol corresponds to the CCM-MEA 10 mg catalysts cm⁻²; triangle symbol – CCS-MEA. Empty symbols refer to the |Z| axis besides the full symbols refer to phase angle (Θ) axis. The full line refers to the fitting curves. EIS maximal amplitude 20 mV, cell voltage 1.8 V, frequency range 65 kHz-1 Hz.

EIS may provide additional information on the properties of the individual MEAs. Due to the fast cathodic reaction and significantly slower anodic reaction, the spectra recorded exhibited only one time constant. Therefore, a simplified or full Randles equivalent circuit was used to evaluate the ohmic resistivity of the cell R_s and the anodic polarization resistance R_p. The values determined are summarized in Fig. 3B. Due to the fact that some of the measured spectra showed only one time constant Fig. 3B shows the overall values of the R_p, i.e. the sum of the R_p(anode) and R_p(cathode) where they were

distinguishable. This can be justified by the minimal values of the $R_p(\text{cathode})$, which were 10 times lower when compared to the $R_p(\text{anode})$. The measured spectra are in the form of Nyquist and Bode plots shown in Fig. 3 C, D.

As can be seen in Fig. 3B, the CCM-MEA catalyst load of 2.5 mg cm^{-2} showed the lowest cell resistivity with the value $0.03 \Omega \text{ cm}^2$. This is in agreement with the above explanation for the superior performance of the CCM-MEA with the lowest catalyst load as being caused by the low resistivity of the catalyst layer. When the CCM-MEA with the catalyst load of 10 mg cm^{-2} and the CCS-MEA are compared, a lower R_s value is determined for the CCS-MEA (0.043 and $0.038 \Omega \text{ cm}^2$ respectively). This is the result of an electric current pathway in the system. In the case of the CCS-MEA, the electric current is distributed through the Ni foam representing the substrate of the catalyst layer. The electron pathway in the less conductive catalyst layer is thus limited to the thickness of the catalyst layer in the direction normal to the surface. In the case of the CCM-MEA, the contact of the catalyst layer to the Ni gas diffusion layer is randomly distributed over the electrode surface. The local current density in the catalyst layer is thus higher and the current lines are distributed not only in the direction normal, but also in the direction lateral to the electrode surface. It has, however, to be borne in mind that this part of the cell ohmic resistivity is negligible when compared to the electrolyte resistivity. The values of the R_p (Fig. 3B) show the same trend with a less significant difference between the CCM-MEA ($10 \text{ mg catalysts cm}^{-2}$) and the CCS-MEA. The lowest value of the R_p was again achieved with the CCM-MEA ($2.5 \text{ mg catalyst cm}^{-2}$). This is in agreement with the discussion of the insufficient conductivity of the catalyst layer impacting its use in the case of excessive thickness.

The impact of liquid electrolyte concentration on the performance of the CCM-MEA in alkaline water electrolysis was investigated for a catalyst loading of 2.5 mg cm^{-2} . The

load curves obtained are shown in Fig. 4. In the case of the lowest KOH concentration of 1 wt.%, a slightly better performance was achieved for the CCS-MEA. The current densities obtained at 2 V were 0.083 and 0.091 A cm⁻² (difference 9.6 %) for CCM-MEA (2.5 mg cm⁻²) and CCS-MEA respectively. At the highest concentration studied, *i.e.* 15 wt.% KOH, the performance is similar for both MEAs (0.179 for CCM-MEA (2.5 mg cm⁻²) and 0.176 A cm⁻² for CCS-MEA). At the same time, Fig. 4 well documents the increase in electrolysis performance with the increasing concentration of the KOH solution used. The increase was about 115.7 % and 93.4 % for CCM-MEA (2.5 mg cm⁻²) and CCS-MEA respectively. This behaviour, connected with an increase in the liquid electrolyte conductivity, is common.

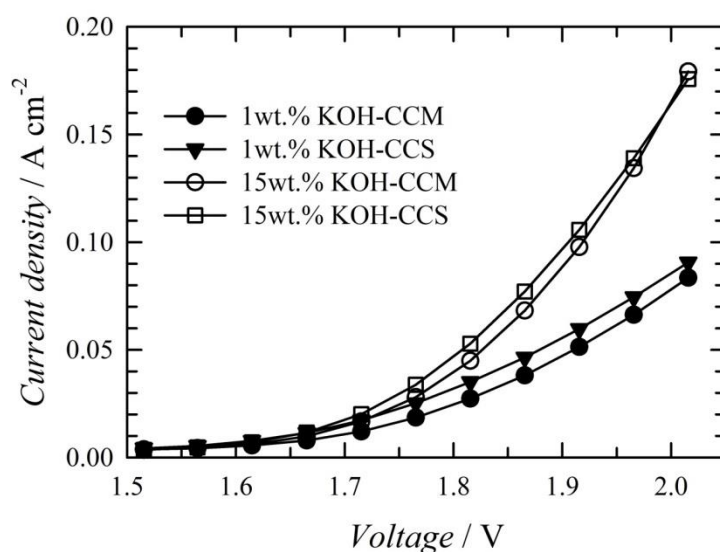


Fig. 4: Load curves of the APWEL using different MEAs (identified in the figure inset) and concentration of the liquid electrolyte (shown in figure inset). Geometrical area of the electrode 4 cm², temperature 45 °C, electrolyte flow rate 5 ml min⁻¹.

The shape of the individual load curves indicates a slower initiation of the water decomposition reaction for CCM-type electrodes, followed by a more rapid increase in the current density at higher loads. However, the traditional plot does not allow a more detailed discussion of this phenomenon. Therefore, in Fig. 5 the load curves are shown in a logarithmic scale providing a more comprehensive insight.

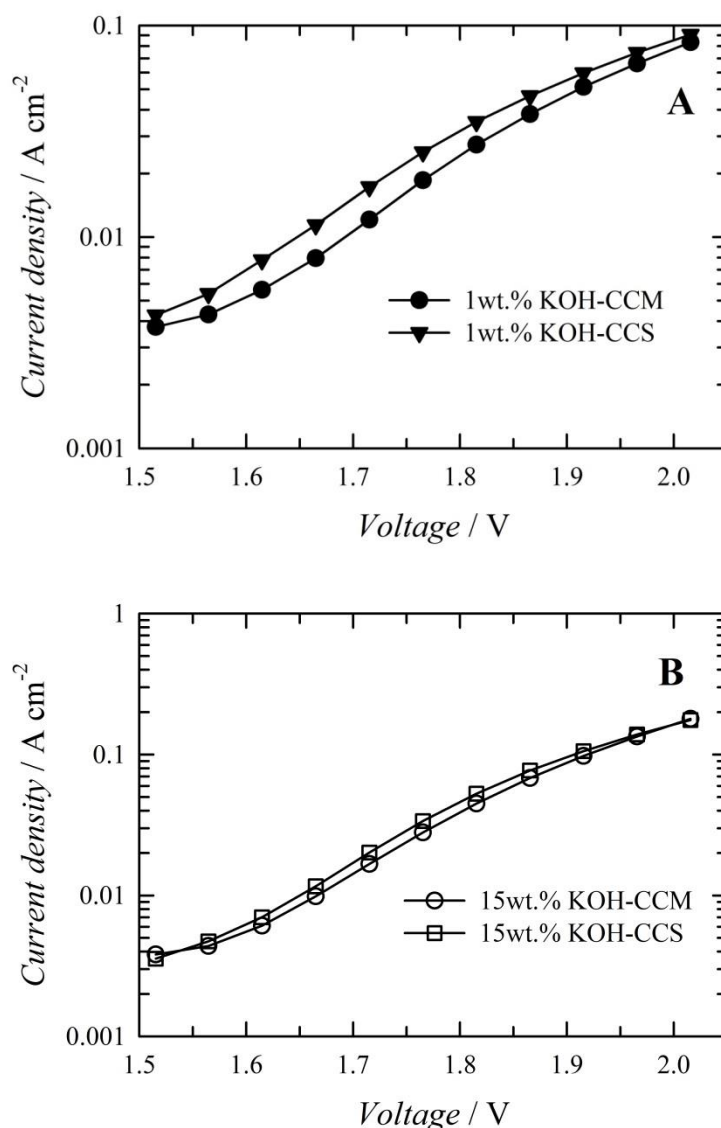


Fig. 5: Detailed analysis of the load curves of the alkaline water electrolysis. Different MEAs and concentration of the liquid electrolyte identified in the figure inset. Geometrical area of the electrode 4 cm², temperature 45 °C, electrolyte flow rate 5 ml min⁻¹.

Fig. 5A shows the load curves recorded using 1wt.% KOH solution as a liquid electrolyte for both MEA configurations. The logarithmic plot confirms that the MEA in the CCS configuration shows faster activation of the water decomposition reaction compared to the CCM-MEA (cell voltage of 1.5 to 1.65 V) as it was able to achieve current density higher about 43.5 % at cell voltage 1.65 V. The reason for this lies in the true value of the electrode potential in different phases. The CCS-MEA is typically represented by a thin layer of catalyst deposited on the surface of the metallic phase of the Ni foam. The electric potential of the catalytic particle can thus be considered to be equal or close to

the potential of the Ni foam substrate itself. In the case of the CCM-MEA, the situation is different. Because of the thickness of the catalytic layers of about 35 μm and their relatively low electrical conductivity, especially in the case of the cathode, the electric potential of the electronic conductor close to the membrane surface, where the reaction primarily takes place, is lower than in the case of the CCS. This has a direct impact on the decrease in the corresponding electrode potential, i.e. the driving force of the electrode reaction. This results in the formally slower initiation of the water decomposition reaction in the case of the CCM-MEA. In the range of cell voltage 1.65 to 1.80 V the values of the current density are parallel to each other and the difference thus remains constant. In the cell voltage range of 1.80 to 2.0 V the slope of the CCM-MEA load curve becomes increasingly higher compared to that of the CCS-MEA. The reason is clearly the better ionic contact between the catalytic layer and the alkaline polymer electrolyte membrane. An analysis of the result obtained using 15 wt. % KOH solution as a circulating liquid electrolyte is shown in Fig. 5B. The nature of the behaviour is identical to the previous case of the more diluted solution. The main change is the significantly less pronounced differences between the individual electrode types when the CCS-MEA over performs CCM-MEA (2.5 mg cm^{-2}) in current density at cell voltage 1.65 V about 17.8 % when compared to 43.5 % for 1wt.% KOH solution. This is evidently due to the higher ionic conductivity of the liquid, as well as the polymer electrolyte. This documents the fact that the potential of the CCM-MEA consists above all in the environment with low conductivity of the circulating media.

It should be remembered that the ratio of the amount of catalyst to the amount of binder in the catalyst layer (9:1) as well as the method and conditions of catalyst layer deposition were optimized for the CCS-MEA. It can be anticipated that careful

optimization of both parameters for the CCM-MEA will bring about an improvement in APWEL performance.

3.3 CCM-MEA durability under electrolysis conditions

In the final step, the stability of the CCM-MEA over time was studied. Fig. 6 shows the cell voltage development during 20 hours of alkaline water electrolysis at 250 mA cm^{-2} . All MEA configurations used showed similar trends. Within the initial 5 hours, the cell voltage slowly increased until it achieved a stable value. This was approximately 2.1 V for the CCS-MEA and the CCM-MEA ($2.5 \text{ mg catalyst cm}^{-2}$) and 2.13 for the CCM-MEA ($10 \text{ mg catalyst cm}^{-2}$). As discussed above, it is possible to see the cross-section of the CCMs after this experiment in Fig. 2B and D without any significant signs of delamination of the catalyst layer in the case of the CCM-MEA ($2.5 \text{ mg catalyst cm}^{-2}$). The duration of this test which lasted 20 hours can still be considered rather short. Nevertheless, Leng *et al.* [50] reported that their CCM-MEA was stable for 27 hours. This is also in line with the results of Ito *et al.* [51] who reported that the MEA was stable for 20 hours. In our case, there were no signs of degradation after the load curve measurement followed by a 20-hour galvanostatic test at a current density of 250 mA cm^{-2} . This definitely indicates the improved stability of the anion selective polymer binder used. This observation was further confirmed by a prolonged (72 hours) test under APWEL conditions, shown in Fig. 7. When the observed performance of the APWEL is compared with the literature, Ito *et al.* achieved similar results when operating at higher temperature (50°C) but in lower pH liquid electrolyte (1wt.% K_2CO_3) with non Pt metals as catalysts for OER and HER. The current density of 0.25 A cm^{-2} was achieved at cell voltage approx. 2.2 V. On the other hand significantly better performance (but with limited stability) was achieved by Lang *et al.* [50] who showed the short-term result of 0.25 A cm^{-2} at approx. 1.7 V. However, this was at the expense of utilization of Pt/C

and IrO_2 as catalyst for HER and OER. Even more, similar as in the case of Ito et al. work, the anion selective polymer binder was not stable at the anode side.

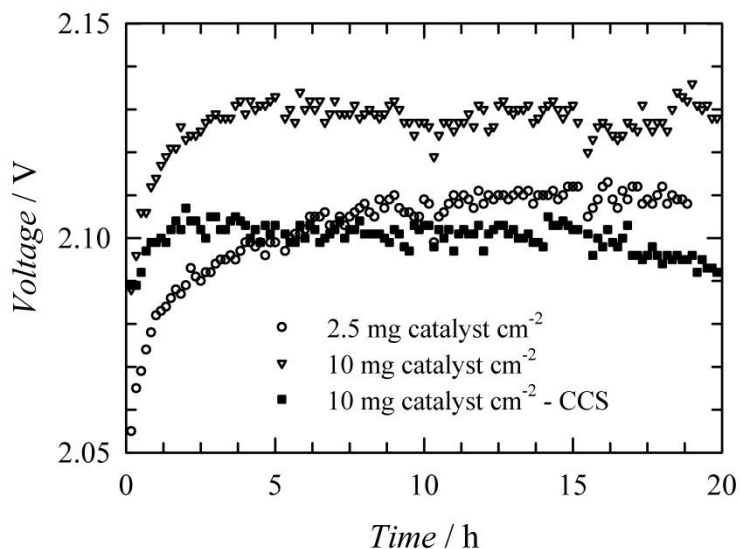


Fig. 6: Dependence of cell voltage on the time of alkaline water electrolysis using different MEAs (shown in figure inset) at current density 250 mA cm^{-2} . Geometrical area of the electrode 4 cm^2 , temperature 45°C , concentration of the liquid electrolyte 10 wt.%, electrolyte flow rate 5 ml min^{-1} .

Fig. 7A shows the 72-hours stability test of the optimized CCM-MEA. Stability test was interrupted in the 20th and the 48th hour in order to investigate the cell behaviour by electrochemical impedance spectroscopy. Due to these interruptions, higher scatter of the cell voltage data is visible on the graph. In average, however, significant changes in cell voltage development were not observed for the CCM-MEA with a catalyst loading of 2.5 mg cm^{-2} . The average value of the cell voltage was $2.097 \pm 0.008 \text{ V}$ ($\pm 0.38 \%$) with the minimum value of 2.060 V and maximum value of 2.108 V . The average value of the cell voltage corresponds to the thermodynamic efficiency of 70 % (related to the thermoneutral voltage of water decomposition 1.48 V at 25°C). High stability of the prepared CCM-MEA is further supported by the evaluation of impedance spectra analysing the values of R_s and R_p , see Fig. 7B. In the case of the PSEBS-CM-DABCO polymer electrolyte degradation, the value R_s should increase due to the decrease in ionic conductivity of the membrane. In case of the catalyst dissolution, degradation or loose,

the R_p value should increase. In present case, however, R_s and R_p were characterised by an initial value of 0.118 and 0.270 Ω respectively. After 72 hours of electrolysis, values have reached 0.108 Ω (R_s) and 0.271 Ω (R_p). Corresponding average values of 0.107 $\Omega \pm 0.007 \Omega$ for R_s and 0.260 $\Omega \pm 0.010 \Omega$ for R_p were achieved. It can thus be concluded, that no clear sign of CCM-MEA degradation was observed. The current density of 0.25 A cm⁻² achieved at 2.1 V might be considered as rather low when compared to the results showing current density > 0.5 A cm⁻² at less 2 V [55, 56], but these are mainly utilizing the precious metals as catalysts. Marinkas *et al.* achieved the current density of 0.3 A cm⁻² using novel anion selective membrane or 0.5 A cm⁻² with commercially available membrane FAA3-PK-75 (Fumatech) in CCS-MEA configuration at cell voltage 1.8 V. However, their system contained 3 mg IrO₂ cm⁻² on anode side and 1.5 Pt/C cm⁻² on cathode side [55], which is in contradictory to assumption of low capital cost of the APWEL due to the utilization of the cheap non platinum metals catalysts. Ito *et al.* used in another work non platinum anode catalyst and Pt/C for HER catalysis. The cathode was prepared as CCM, but for anode preparation CCS approach was used due to the limited stability of the polymer anion selective binder. In the new study [56] the current density of 0.25 A cm⁻² was achieved at cell voltage approx. 1.75 V. The only difference between this value and value of the cell voltage 2.2 V achieved for 0.25 A cm⁻² published in the previous work [51] is the replacement of the non-platinum catalyst for Pt/C (1.8 mg Pt cm⁻²) on cathode side. When non precious catalysts are considered, the achieved current density is somewhere in between of the published values [57-59]. For example Zeng *et al.* achieved maximum current density of 0.208 A cm⁻² at 70 °C with 0.1 mol dm⁻³ NaOH electrolyte using CuCo_x and Ni/(CeO₂-La₂O₃) catalysts as anode and cathode respectively at cell voltage 2.2 V [59]. In another work, Borisov *et al.* [60] used Ni and Co based monometallic catalysts on titanium suboxide carrier resulting in current density

of 0.2 A cm^{-2} at 2.0 V and temperature $80 \text{ }^{\circ}\text{C}$ with PBI membrane doped by 50wt.% KOH. In all of these cases, the performance of the APWEL presented in this work is showing better results.

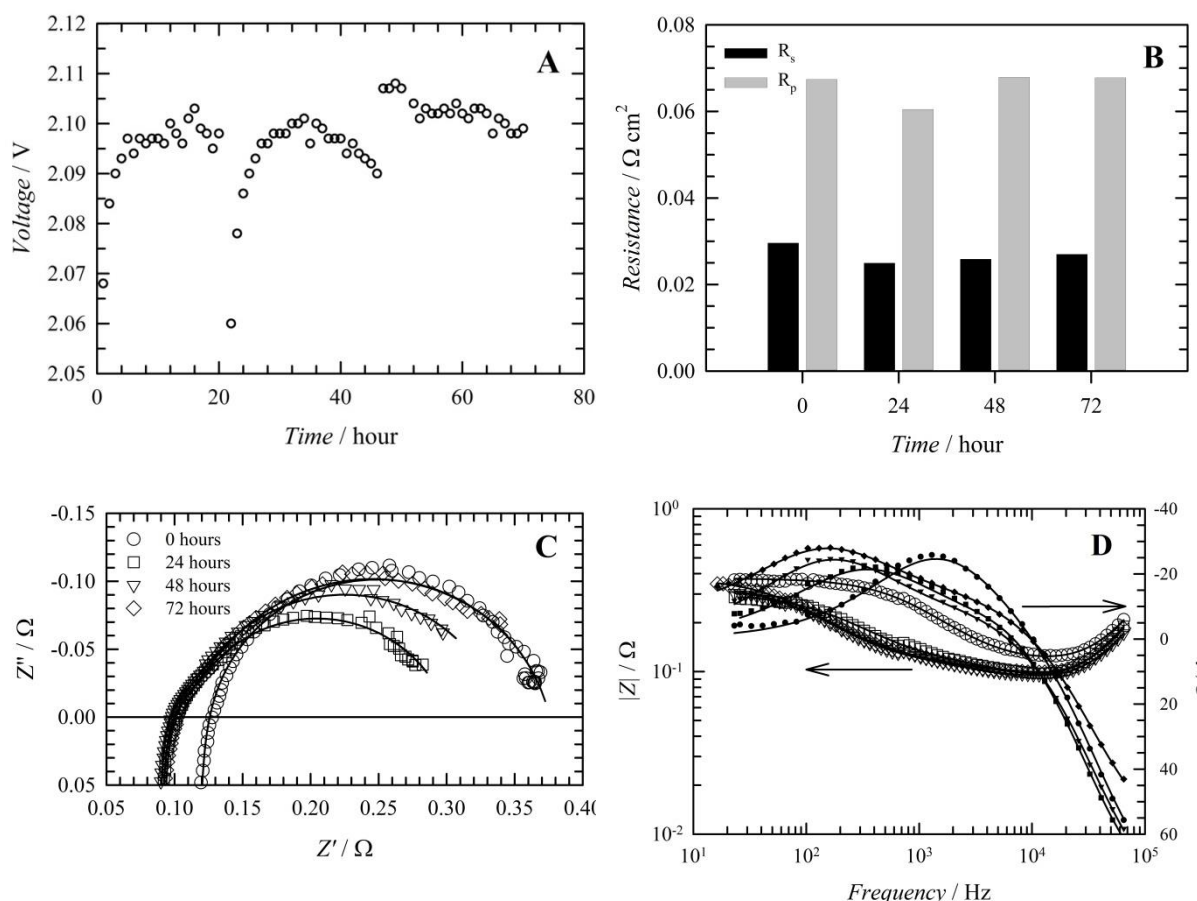


Fig. 7: Dependence of the (A) cell voltage and (B) solution and polarization resistance on time of the APWEL using different MEAs (identified in the figure inset) at a current density of 250 mA cm^{-2} . Geometrical area of the electrode 4 cm^2 , temperature $45 \text{ }^{\circ}\text{C}$, concentration of the liquid electrolyte 10 wt.%, electrolyte flow rate 5 ml min^{-1} . (C) Nyquist plot; (D) Bode plot – circle symbol corresponds to the CCM-MEA $2.5 \text{ mg catalysts cm}^{-2}$; square symbol corresponds to the CCM-MEA $10 \text{ mg catalysts cm}^{-2}$; triangle symbol – CCS-MEA. Empty symbols refer to the $|Z|$ axis besides the full symbols refer to phase angle (Θ) axis. EIS maximal amplitude 20 mV, cell voltage 1.8 V, frequency range 65 kHz-1 Hz.

Besides this, surface characterisation of the anode and cathode from the point of view of the morphological and elemental changes have been performed using SEM, EDX and ICP-OES analysis. The images of both surface before and after extended experiments are shown in Fig. 8 and Fig. 9.

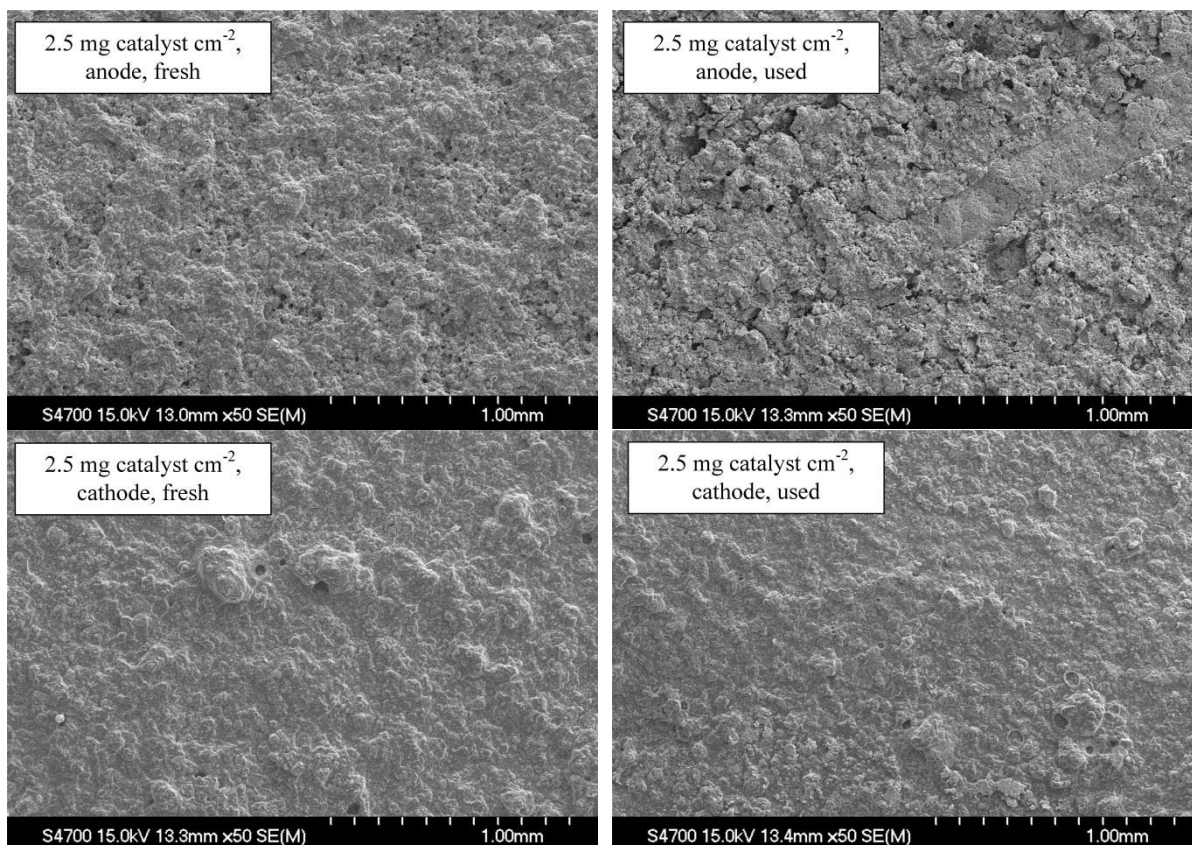


Fig. 8: Images of the surfaces of the deposited anode and cathode at catalyst load 2.5 mg cm^{-2} prior and after extended APWEL experiment. Conditions of the APWEL: current density of 250 mA cm^{-2} , geometrical area of the electrode 4 cm^2 , temperature 45°C , concentration of the liquid electrolyte $10 \text{ wt.}\%$, electrolyte flow rate 5 ml min^{-1} .

From the images shown in Fig. 8 is apparent high mechanical stability of both catalyst layers anode and cathode. In the case of the anode catalyst layer after 72 hours of APWEL, some changes in morphology of the surface can be seen, however, this can be attributed to the influence of the Ni foam, which was pressed to the layer. In the case of the cathode layer, no changes in the morphology of the layer are visible when the image prior to and after the 72 hours of APWEL. When anode and cathode layers are compared with each other, the cathode layers are more compact, besides anode catalyst layers show higher degree of porosity. The similar is possible to see from Fig. 9 where the layers with higher used catalyst load (10 mg cm^{-2}) are shown. However, in this case the morphology of the anode side after 72 hours of APWEL seems to be more influenced. This can be due to higher pressure inside the catalyst layer due to the gas evolution. For the cathode, the surface seems to be more wrinkled after APWEL. When

the images from Fig. 8 and Fig. 9 are compared, CCM-MEA with $2.5 \text{ mg catalyst cm}^{-2}$ is showing higher stability of the catalyst layers.

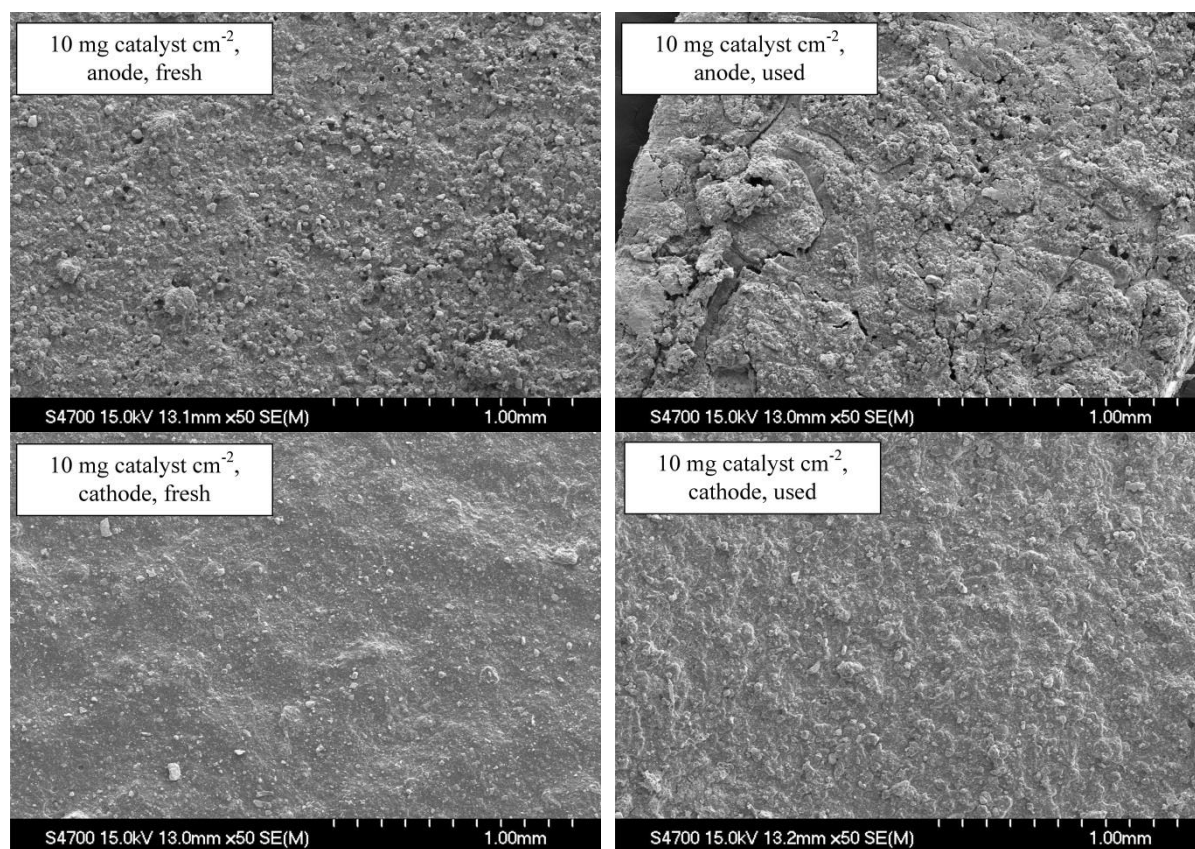


Fig. 9: Images of the surfaces of the deposited anode and cathode at catalyst load 10 mg cm^{-2} prior and after extended APWEL experiment. Conditions of the APWEL: current density of 250 mA cm^{-2} , geometrical area of the electrode 4 cm^2 , temperature 45°C , concentration of the liquid electrolyte $10 \text{ wt.}\%$, electrolyte flow rate 5 ml min^{-1} .

The EDX analysis of the surfaces of the anodes and cathodes were investigated in order to obtain information on the element changes during 72 hours of APWEL experiment. Results of EDX analysis are summarized in Table 1. From the data shown it is possible to see that the thickness of the catalyst layer (catalyst load) has no impact on the composition of the catalyst layer. However, it is possible to see the differences in the composition of the fresh catalyst layers and the layers after 72 hours APWEL. In order to exclude the possibility of the dissolution of the catalysts into the electrolyte solution the KOH solution after the 72 hours APWEL were investigated by ICP-OES. The calibration curve used for evaluation allowed to detect the Ni, Co or Fe in minimal concentration 1 ppm . However, none of the listed elements was detected.

It is thus possible to conclude that the changes are due to the differences in local composition of the catalyst layer and the sensitivity of the experimental technique.

Table 1: Composition of the deposited catalyst layers of CCM-MEA observed by EDX.

Layer	Catalyst load mg cm ⁻²	State	Ni at.	Co at.	Fe at.	Ratio Co/Ni	Ratio Fe/Ni
Anode	2.5	Fresh	0.99	2.00	-	2.02	-
Anode	2.5	Used	0.88	2.12	-	2.40	-
Cathode	2.5	Fresh	0.84	-	2.16	-	2.56
Cathode	2.5	Used	0.91	-	2.09	-	2.30
Anode	10	Fresh	0.99	2.01	-	2.03	-
Anode	10	Used	0.92	2.08	-	2.25	-
Cathode	10	Fresh	0.86	-	2.03	-	2.48
Cathode	10	Used	0.93	-	2.25	-	2.24

4 Conclusions

Using an anion-selective polymer membrane based on a block copolymer of styrene-ethylene-butylene-styrene and its 5 wt.% solution in chloroform, a stable catalyst-coated membrane assembly for alkaline water electrolysis utilizing non-platinum catalysts was prepared. Scanning electron microscopy revealed good contact between the catalyst layers and the membrane. The preliminary results of the alkaline water electrolysis cell revealed both a promising performance and the stability of this assembly, although further optimisation of the CCM materials and preparation method are envisaged. Even at this stage, however, the catalyst load can be reduced by 75 % (from 10 to 2.5 mg cm⁻²) with no negative impact on the alkaline water electrolysis performance compared to a traditional, catalyst-coated substrate. The next efforts will focus on optimization of the composition of the catalyst layers and verification of the stability of the CCM-MEA under longer and dynamic operating conditions.

Acknowledgement

The financial support of this research received from the Grant Agency of the Czech Republic under project No. 16-20728S is gratefully acknowledged. Equipment purchased within the Framework of the Operational Programme Prague – Competitiveness (CZ.2.16/3.1.00/24501) and “National Program of Sustainability“ (NPU I LO1613) MSMT-43760/2015) contributed towards achieving the aims of this study. Ramato A. Tufa acknowledges the financial support of the European Union’s Horizon 2020 Research and innovation programme under the Marie Skłodowska-Curie Actions IF Grant agreement No. 748683.

5 Literature

- [1] L. Xiao, S. Zhang, J. Pan, C. Yang, M. He, L. Zhuang, J. Lu, First implementation of alkaline polymer electrolyte water electrolysis working only with pure water, *Energy & Environmental Science*, 5 (2012) 7869-7871.
- [2] D. Pletcher, X. Li, Prospects for alkaline zero gap water electrolyzers for hydrogen production, *International Journal of Hydrogen Energy*, 36 (2011) 15089-15104.
- [3] D. Chanda, J. Hnat, A.S. Dobrota, I.A. Pasti, M. Paidar, K. Bouzek, The effect of surface modification by reduced graphene oxide on the electrocatalytic activity of nickel towards the hydrogen evolution reaction, *Physical Chemistry Chemical Physics*, 17 (2015) 26864-26874.
- [4] A. Gabler, C.I. Müller, T. Rauscher, M. Köhring, B. Kieback, L. Röntzsch, W. Schade, Ultrashort pulse laser-structured nickel surfaces as hydrogen evolution electrodes for alkaline water electrolysis, *International Journal of Hydrogen Energy*, 42 (2017) 10826-10833.
- [5] D. Chanda, J. Hnat, M. Paidar, J. Schauer, K. Bouzek, Synthesis and characterization of NiFe₂O₄ electrocatalyst for the hydrogen evolution reaction in alkaline water electrolysis using different polymer binders, *Journal of Power Sources*, 285 (2015) 217-226.
- [6] M.S. Balogun, W. Qiu, Y. Huang, H. Yang, R. Xu, W. Zhao, G.R. Li, H. Ji, Y. Tong, Cost-Effective Alkaline Water Electrolysis Based on Nitrogen-and Phosphorus-Doped Self-Supportive Electrocatalysts, *Advanced Materials*, 29 (2017).
- [7] J. Hnat, M. Plevová, J. Žitka, M. Paidar, K. Bouzek, Anion-selective materials with 1,4-diazabicyclo[2.2.2]octane functional groups for advanced alkaline water electrolysis, *Electrochimica Acta*, 248 (2017) 547-555.
- [8] D. Aili, M.K. Hansen, R.F. Renzaho, Q. Li, E. Christensen, J.O. Jensen, N.J. Bjerrum, Heterogeneous anion conducting membranes based on linear and crosslinked KOH doped polybenzimidazole for alkaline water electrolysis, *Journal of Membrane Science*, 447 (2013) 424-432.
- [9] J.R. Varcoe, P. Atanassov, D.R. Dekel, A.M. Herring, M.A. Hickner, P.A. Kohl, A.R. Kucernak, W.E. Mustain, K. Nijmeijer, K. Scott, T. Xu, L. Zhuang, Anion-exchange membranes in electrochemical energy systems, *Energy & Environmental Science*, 7 (2014) 3135-3191.

- [10] T. Rauscher, C.I. Bernäcker, U. Mühle, B. Kieback, L. Röntzsch, The effect of Fe as constituent in Ni-base alloys on the oxygen evolution reaction in alkaline solutions at high current densities, *International Journal of Hydrogen Energy*, 44 (2019) 6392-6402.
- [11] K.I. Siwek, S. Eugénio, D.M.F. Santos, M.T. Silva, M.F. Montemor, 3D nickel foams with controlled morphologies for hydrogen evolution reaction in highly alkaline media, *International Journal of Hydrogen Energy*, 44 (2019) 1701-1709.
- [12] S. Wang, X. Zou, Y. Lu, S. Rao, X. Xie, Z. Pang, X. Lu, Q. Xu, Z. Zhou, Electrodeposition of nano-nickel in deep eutectic solvents for hydrogen evolution reaction in alkaline solution, *International Journal of Hydrogen Energy*, 43 (2018) 15673-15686.
- [13] Y. Ali, V.-T. Nguyen, N.-A. Nguyen, S. Shin, H.-S. Choi, Transition-metal-based NiCoS/C-dot nanoflower as a stable electrocatalyst for hydrogen evolution reaction, *International Journal of Hydrogen Energy*, 44 (2019) 8214-8222.
- [14] S. Ma, L. Wang, S. Zhang, H. Jin, M. Wan, Y. Pan, T. Zhang, Y. Wen, M. Zhang, H. Zhu, M. Du, Facile fabrication of a binary NiCo phosphide with hierarchical architecture for efficient hydrogen evolution reactions, *International Journal of Hydrogen Energy*, 44 (2019) 4188-4196.
- [15] B.X. Tao, C. Ye, X.L. Li, X.H. Wang, G. Chen, L.J. Li, H.Q. Luo, N.B. Li, Heterogeneous cobalt phosphides nanoparticles anchored on carbon cloth realizing the efficient hydrogen generation reaction, *International Journal of Hydrogen Energy*, 44 (2019) 531-539.
- [16] N. Xu, G. Cao, L. Gan, Z. Chen, M. Zang, H. Wu, P. Wang, Carbon-coated cobalt molybdenum oxide as a high-performance electrocatalyst for hydrogen evolution reaction, *International Journal of Hydrogen Energy*, 43 (2018) 23101-23108.
- [17] M.R. Kraglund, D. Aili, K. Jankova, E. Christensen, Q. Li, J.O. Jensen, Zero-gap alkaline water electrolysis using ion-solvating polymer electrolyte membranes at reduced KOH concentrations, *Journal of The Electrochemical Society*, 163 (2016) F3125-F3131.
- [18] D. Burnat, M. Schlupp, A. Wichser, B. Lothenbach, M. Gorbar, A. Züttel, U.F. Vogt, Composite membranes for alkaline electrolysis based on polysulfone and mineral fillers, *Journal of Power Sources*, 291 (2015) 163-172.
- [19] M. Carmo, D.L. Fritz, J. Mergel, D. Stolten, A comprehensive review on PEM water electrolysis, *International Journal of Hydrogen Energy*, 38 (2013) 4901-4934.
- [20] A. Lindermeir, G. Rosenthal, U. Kunz, U. Hoffmann, On the question of MEA preparation for DMFCs, *Journal of Power Sources*, 129 (2004) 180-187.
- [21] I.-S. Park, W. Li, A. Manthiram, Fabrication of catalyst-coated membrane-electrode assemblies by doctor blade method and their performance in fuel cells, *Journal of Power Sources*, 195 (2010) 7078-7082.
- [22] Y.-H. Cho, H.-S. Park, Y.-H. Cho, I.-S. Park, Y.-E. Sung, The improved methanol tolerance using Pt/C in cathode of direct methanol fuel cell, *Electrochimica Acta*, 53 (2008) 5909-5912.
- [23] C.S. Kim, Y.G. Chun, D.H. Peck, D.R. Shin, A novel process to fabricate membrane electrode assemblies for proton exchange membrane fuel cells, *International Journal of Hydrogen Energy*, 23 (1998) 1045-1048.
- [24] L.J. Hobson, Y. Nakano, H. Ozu, S. Hayase, Targeting improved DMFC performance, *Journal of Power Sources*, 104 (2002) 79-84.
- [25] D. Bevers, N. Wagner, M. Von Bradke, Innovative production procedure for low cost PEFC electrodes and electrode/membrane structures, *International Journal of Hydrogen Energy*, 23 (1998) 57-63.
- [26] Y.-G. Chun, C.-S. Kim, D.-H. Peck, D.-R. Shin, Performance of a polymer electrolyte membrane fuel cell with thin film catalyst electrodes, *Journal of Power Sources*, 71 (1998) 174-178.
- [27] M.B. Sassin, Y. Garsany, B.D. Gould, K.E. Swider-Lyons, Fabrication Method for Laboratory-Scale High-Performance Membrane Electrode Assemblies for Fuel Cells, *Analytical Chemistry*, 89 (2017) 511-518.

- [28] Y.-C. Park, H. Tokiwa, K. Kakinuma, M. Watanabe, M. Uchida, Effects of carbon supports on Pt distribution, ionomer coverage and cathode performance for polymer electrolyte fuel cells, *Journal of Power Sources*, 315 (2016) 179-191.
- [29] S. Shukla, K. Domican, K. Karan, S. Bhattacharjee, M. Secanell, Analysis of Low Platinum Loading Thin Polymer Electrolyte Fuel Cell Electrodes Prepared by Inkjet Printing, *Electrochimica Acta*, 156 (2015) 289-300.
- [30] S. Shukla, D. Stanier, M. Saha, J. Stumper, M. Secanell, Analysis of inkjet printed pefc electrodes with varying platinum loading, *Journal of The Electrochemical Society*, 163 (2016) F677-F687.
- [31] L. Sun, R. Ran, Z. Shao, Fabrication and evolution of catalyst-coated membranes by direct spray deposition of catalyst ink onto Nafion membrane at high temperature, *International Journal of Hydrogen Energy*, 35 (2010) 2921-2925.
- [32] C.H. Hsu, C.C. Wan, An innovative process for PEMFC electrodes using the expansion of Nafion film, *Journal of Power Sources*, 115 (2003) 268-273.
- [33] A.S. Alavijeh, R.M. Khorasany, Z. Nunn, A. Habisch, M. Lauritzen, E. Rogers, G.G. Wang, E. Kjeang, Microstructural and mechanical characterization of catalyst coated membranes subjected to in situ hygrothermal fatigue, *Journal of The Electrochemical Society*, 162 (2015) F1461-F1469.
- [34] R. Alink, M. Schüßler, M. Pospischil, D. Erath, D. Gerteisen, Analyzing the influence of high electrode potentials on intrinsic properties of catalyst coated membranes using impedance spectroscopy, *Journal of Power Sources*, 327 (2016) 526-534.
- [35] S. Haase, M. Moser, J. Hirschfeld, K. Jozwiak, Current density and catalyst-coated membrane resistance distribution of hydro-formed metallic bipolar plate fuel cell short stack with 250 cm² active area, *Journal of Power Sources*, 301 (2016) 251-260.
- [36] K.-H. Kim, K.-Y. Lee, H.-J. Kim, E. Cho, S.-Y. Lee, T.-H. Lim, S.P. Yoon, I.C. Hwang, J.H. Jang, The effects of Nafion® ionomer content in PEMFC MEAs prepared by a catalyst-coated membrane (CCM) spraying method, *International Journal of Hydrogen Energy*, 35 (2010) 2119-2126.
- [37] X. Leimin, L. Shijun, Y. Lijun, L. Zhenxing, Investigation of a Novel Catalyst Coated Membrane Method to Prepare Low-Platinum-Loading Membrane Electrode Assemblies for PEMFCs, *Fuel Cells*, 9 (2009) 101-105.
- [38] M.K. Debe, A.K. Schmoedel, G.D. Vernstrom, R. Atanasoski, High voltage stability of nanostructured thin film catalysts for PEM fuel cells, *Journal of Power Sources*, 161 (2006) 1002-1011.
- [39] H. Yu, C. Ziegler, M. Oszcipok, M. Zobel, C. Hebling, Hydrophilicity and hydrophobicity study of catalyst layers in proton exchange membrane fuel cells, *Electrochimica Acta*, 51 (2006) 1199-1207.
- [40] V.O. Mittal, H.R. Kunz, J.M. Fenton, Effect of catalyst properties on membrane degradation rate and the underlying degradation mechanism in PEMFCs, *Journal of The Electrochemical Society*, 153 (2006) A1755-A1759.
- [41] M.T. Stocker, B.M. Barnes, M. Sohn, E. Stanfield, R.M. Silver, Development of large aperture projection scatterometry for catalyst loading evaluation in proton exchange membrane fuel cells, *Journal of Power Sources*, 364 (2017) 130-137.
- [42] H. Tang, S. Wang, M. Pan, S.P. Jiang, Y. Ruan, Performance of direct methanol fuel cells prepared by hot-pressed MEA and catalyst-coated membrane (CCM), *Electrochimica Acta*, 52 (2007) 3714-3718.
- [43] X. Yan, S. Gu, G. He, X. Wu, J. Benziger, Imidazolium-functionalized poly(ether ether ketone) as membrane and electrode ionomer for low-temperature alkaline membrane direct methanol fuel cell, *Journal of Power Sources*, 250 (2014) 90-97.
- [44] C. Wannek, S. Nehr, M. Vahlenkamp, J. Mergel, D. Stolten, Pseudo-half-cell measurements on symmetrical catalyst-coated membranes and their relevance for optimizing DMFC anodes, *J Appl Electrochem*, 40 (2009) 29.

- [45] M. Debe, S. Hendricks, G. Vernstrom, M. Meyers, M. Brostrom, M. Stephens, Q. Chan, J. Willey, M. Hamden, C.K. Mittelsteadt, Initial performance and durability of ultra-low loaded NSTF electrodes for PEM electrolyzers, *Journal of the Electrochemical Society*, 159 (2012) K165-K176.
- [46] J. Mo, S. Steen, Z. Kang, G. Yang, D.A. Taylor, Y. Li, T.J. Toops, M.P. Brady, S.T. Retterer, D.A. Cullen, Study on corrosion migrations within catalyst-coated membranes of proton exchange membrane electrolyzer cells, *International Journal of Hydrogen Energy*, 42 (2017) 27343-27349.
- [47] K.E. Ayers, J.N. Renner, N. Danilovic, J.X. Wang, Y. Zhang, R. Maric, H. Yu, Pathways to ultra-low platinum group metal catalyst loading in proton exchange membrane electrolyzers, *Catalysis Today*, 262 (2016) 121-132.
- [48] V.K. Puthiyapura, M. Mamlouk, S. Pasupathi, B.G. Pollet, K. Scott, Physical and electrochemical evaluation of ATO supported IrO₂ catalyst for proton exchange membrane water electrolyser, *Journal of Power Sources*, 269 (2014) 451-460.
- [49] H. Gasteiger, S. Yan, Dependence of PEM fuel cell performance on catalyst loading, *Journal of Power Sources*, 127 (2004) 162-171.
- [50] Y. Leng, G. Chen, A.J. Mendoza, T.B. Tighe, M.A. Hickner, C.-Y. Wang, Solid-State Water Electrolysis with an Alkaline Membrane, *Journal of the American Chemical Society*, 134 (2012) 9054-9057.
- [51] H. Ito, N. Miyazaki, S. Sugiyama, M. Ishida, Y. Nakamura, S. Iwasaki, Y. Hasegawa, A. Nakano, Investigations on electrode configurations for anion exchange membrane electrolysis, *Journal of Applied Electrochemistry*, 48 (2018) 305-316.
- [52] J. Hnát, M. Plevová, J. Žitka, M. Paidar, K. Bouzek, Anion-selective materials with 1,4-diazabicyclo[2.2.2]octane functional groups for advanced alkaline water electrolysis, *Electrochimica Acta*, 248 (2017) 547-555.
- [53] D. Chanda, J. Hnát, T. Bystron, M. Paidar, K. Bouzek, Optimization of synthesis of the nickel-cobalt oxide based anode electrocatalyst and of the related membrane-electrode assembly for alkaline water electrolysis, *Journal of Power Sources*, 347 (2017) 247-258.
- [54] R.A. Tufa, E. Rugiero, D. Chanda, J. Hnát, W. van Baak, J. Veerman, E. Fontananova, G. Di Profio, E. Drioli, K. Bouzek, E. Curcio, Salinity gradient power-reverse electrodialysis and alkaline polymer electrolyte water electrolysis for hydrogen production, *Journal of Membrane Science*, 514 (2016) 155-164.
- [55] A. Marinkas, I. Strużyńska-Piron, Y. Lee, A. Lim, H.S. Park, J.H. Jang, H.-J. Kim, J. Kim, A. Maljusch, O. Conradi, D. Henkensmeier, Anion-conductive membranes based on 2-mesitylbenzimidazolium functionalised poly(2,6-dimethyl-1,4-phenylene oxide) and their use in alkaline water electrolysis, *Polymer*, 145 (2018) 242-251.
- [56] H. Ito, N. Kawaguchi, S. Someya, T. Munakata, N. Miyazaki, M. Ishida, A. Nakano, Experimental investigation of electrolytic solution for anion exchange membrane water electrolysis, *International Journal of Hydrogen Energy*, 43 (2018) 17030-17039.
- [57] C.C. Pavel, F. Cecconi, C. Emiliani, S. Santiccioli, A. Scaffidi, S. Catanorchi, M. Comotti, Highly Efficient Platinum Group Metal Free Based Membrane-Electrode Assembly for Anion Exchange Membrane Water Electrolysis, *Angewandte Chemie International Edition*, 53 (2014) 1378-1381.
- [58] M. Gong, D.-Y. Wang, C.-C. Chen, B.-J. Hwang, H. Dai, A mini review on nickel-based electrocatalysts for alkaline hydrogen evolution reaction, *Nano Research*, 9 (2016) 28-46.
- [59] L. Zeng, T.S. Zhao, Integrated inorganic membrane electrode assembly with layered double hydroxides as ionic conductors for anion exchange membrane water electrolysis, *Nano Energy*, 11 (2015) 110-118.
- [60] G. Borisov, H. Penchev, K. Maksimova-Dimitrova, F. Ublekov, E. Lefterova, V. Sinigersky, E. Slavcheva, Alkaline water electrolysis facilitated via non-precious monometallic catalysts combined with highly KOH doped polybenzimidazole membrane, *Materials Letters*, 240 (2019) 144-146.

